THE ASTROPHYSICAL JOURNAL, **257**:116–124, 1982 June 1

WOLF-RAYET STARS IN THE MAGELLANIC CLOUDS. II. THE PECULIAR ECLIPSING BINARY HD 5980 IN THE SMC[1]

JACQUES BREYSACHER
European Southern Observatory
ANTHONY F. J. MOFFAT[2]
Département de Physique, Université de Montréal
AND
VIRPI S. NIEMELA[2,3]
Instituto de Astronomia y Fisica del Espacio, and Instituto Argentino de Radioastronomia
Received 1981 May 12; accepted 1981 November 19

ABSTRACT

Over seventy spectra from two observatories are combined to study this eclipsing W-R binary, which has components of type WN4 + O7 I:. The orbital period, $P = 19^{\mathrm{d}}.266 \pm 0^{\mathrm{d}}.003$, and the high eccentricity, $e = 0.49 \pm 0.10$, are confirmed. The width of the strongest optical emission line, He II 4686, decreases by at least a factor of 2 at each eclipse. This is tentatively interpreted in terms of phase-dependent variations of a combination of emission from the W-R envelope as a whole, a hot localized region in the W-R envelope, and the O component wind. Radial velocity variations of He II 4686 probably do not reflect the true W-R orbit; assumption of a mass ratio similar to those observed for other early-WN binaries, along with the more reliable absorption-line orbit of the O component, yield minimum masses of 8 $M_{\odot}$ for the W-R star and 27 $M_{\odot}$ for the O-star.

Subject headings: galaxies: Magellanic Clouds — stars: eclipsing binaries — stars: individual — stars: Wolf-Rayet

I. INTRODUCTION

The star HD 5980, which is probably associated with NGC 346, the largest H II region + OB star cluster in the Small Magellanic Cloud (SMC), was considered by Feast, Thackeray, and Wesselink (1960) to be spectroscopically similar to Wolf-Rayet (W-R) stars but definitely peculiar, with strongly suspected spectral variations. Smith (1968*b*) classified this star as OB + WN and suspected it to be variable in brightness. Walborn (1977) proposed OB? + WN3, and Breysacher and Westerlund (1978) confirmed the existence of spectral variations, assigning it a type WN3p + OB. With an absolute magnitude $M_v = -7.5$ (Azzopardi and Breysacher 1979), HD 5980 is too luminous to be a single W-R star of the hot N sequence according to Smith's (1973) calibration. The eclipsing nature of the object was discovered by Hoffmann, Stift, and Moffat (1978) and the period, $P = 19^{\mathrm{d}}.266$, was determined by Breysacher and Perrier (1980). The light curve reveals a strongly eccentric orbit ($e = 0.47$ for $i = 80°$).

This relatively long period together with the large eccentricity certainly make HD 5980 a potentially interesting object in which to study the structure of a W-R envelope. In particular, since the distance of the two components changes along the orbit, one might expect to observe variable interaction effects between the W-R star and the O companion, nonexistent in the case of circular orbits. The light curve shows that we are dealing with a rather complex system; to understand HD 5980 better, an analysis of the existing spectroscopic data is therefore essential.

[1] Based partly on observations collected at the European Southern Observatory.

[2] Visiting Astronomer, Cerro Tololo Inter-American Observatory, Chile, which is supported by the National Science Foundation.

[3] Member of Carrera del Investigador Cientifico, C.I.C. Prov. de Buenos Aires, Argentina.

II. OBSERVATIONS AND REDUCTIONS

Spectra of different sources are considered here; in chronological order they are:

1. A series of 43 spectrograms obtained during the period 1975 September–1978 October by J. B. at the ESO 1.5 m telescope on La Silla, Chile, with the "Echelec." The echelle spectrograph was used in a low dispersion mode by omitting the cross disperser (a transmission grating) and replacing the echelle grating by a first-order grating. The resulting dispersion is 124 Å mm^{-1} in the blue, in the focal plane of a Lallemand-Duchesne "caméra électronique." For further instrumental details the reader is referred to the article by Baranne and Duchesne (1976). The spectra were secured on Kodak Industrex Type A film and widened to 0.30 mm. The useful spectral range is from λ3900 to λ5400 Å.

2. A series of 28 spectrograms obtained by A. F. J. M., V. S. N., and R. Mendez from 1978 December to 1980 January, using the Carnegie image tube attached to the

1.0 m Yale telescope on Cerro Tololo, Chile. The spectra cover the usable range of $\sim$3700–5000 Å at 45 Å mm^{-1}. Plates 2418–2461 and 3284–3329 are 0.6 mm wide on IIa-O, the plates 3072–3081 with 0.6 mm widening on IIIa-J emulsion, the rest on IIIa-J emulsion with 1.0 mm widening, all baked in forming gas.

3. One spectrogram obtained on 1979 September 28 by J. B. with the Boller and Chivens Cassegrain spectrograph equipped with an Image Dissector Scanner (IDS), at the ESO 3.6 m telescope. The spectral range covered is $\lambda\lambda$4000–7250 with a dispersion of 170 Å mm^{-1}.

Tracings and radial velocity measurements of the first series of spectrograms were made at the INAG "Centre de Dépouillement des Clichés Astronomiques" using a PDS microdensitometer. The second series of spectrograms was measured for radial velocity using the PDS at the David Dunlap Observatory (the first 18 spectrograms) and the Grant machine at the Instituto de Astronomía y Física del Espacio, Buenos Aires (the rest of the spectrograms). For the former, a parabola was fitted through the central half of each line profile; in particular, only the central 26 Å for He II λ4686.

III. DATA ANALYSIS

a) Description of the Spectrum

Figure 1 shows the PDS mean spectrum of HD 5980 obtained from the first nine plates in Table 2.

The strong λ4686 He II emission, which dominates the spectrum, varies in strength and width as a function of the orbital phase (see § III*d*). The $\lambda\lambda$4604–4620 N V and λ4058 N IV emission features have similar intensities, while λ4640 of N III is very weak, suggesting a WN4 type according to Smith's (1968*a*) classification system. This is also supported by the presence of the $\lambda\lambda$7109–7123 emission feature identified as due to N IV by Swings and Jose (1950) and used by Breysacher (1981) to discriminate between the WN3 and WN4 subclasses. The relative

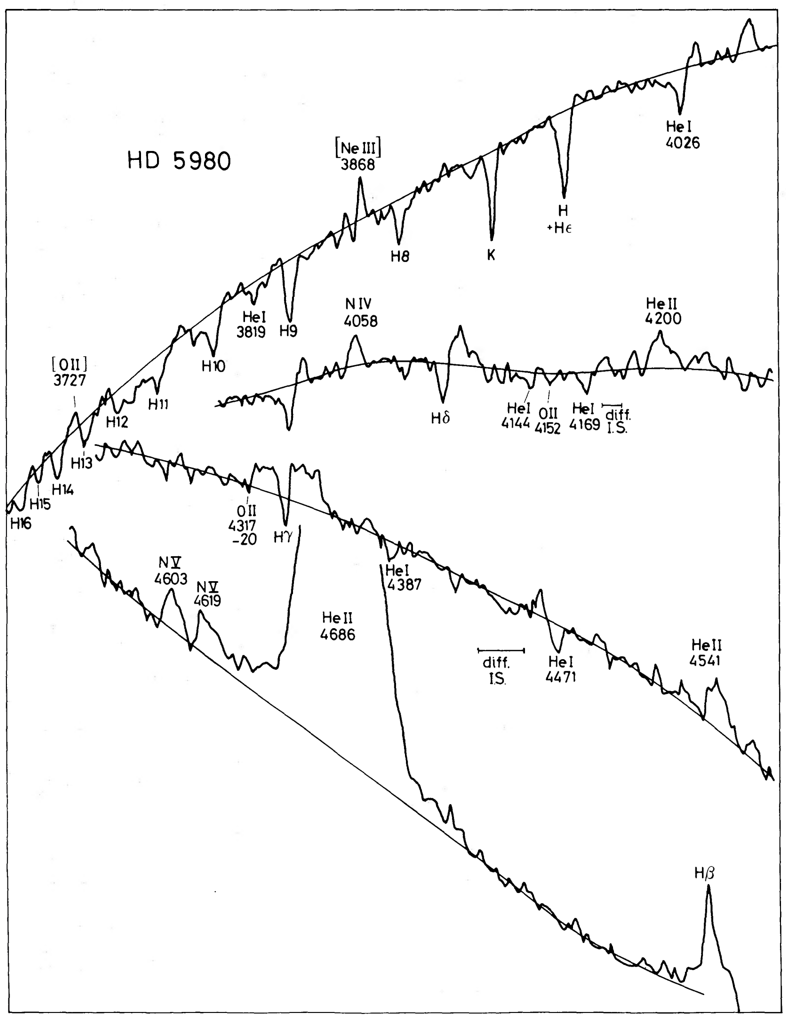

FIG. 1.—PDS mean density of the first nine spectra in Table 2. The narrow emission lines arise in the surrounding nebulosity NGC 346. An attempt has been made to lay a curved line to represent the continuum.

strengths of the He II Pickering emission lines indicate that the H/He ratio is probably low.

The absorption spectrum is very much like the one of the O component in SMC/AB 6 (Azzopardi and Breysacher 1979) classified WN3 + O7 I: and only 0.4 mag fainter than HD 5980 = SMC/AB 5. The ratio He II 4541/He I 4471 has a value of about unity which suggests a spectral type O7 here too, and the line widths appear normal for O stars.

The resulting classification of HD 5980 is thus: WN4 + O7 I:, although the O component may have significant emission at He II 4686 (cf. § IV). The O component thus resembles the nearby star Sk 80 of type O7 Iaf+, which is one of the only two known Of stars in the SMC (Walborn 1978).

The nebular lines observed at λ3727 [O II], λ3869 [Ne III] (relatively strong), Hγ, Hβ, $\lambda\lambda$4959 and 5007 [O III] indicate a fairly high exitation and are due to NGC 346.

The interstellar Ca II lines are present (K component quite strong) and diffuse interstellar bands are also seen.

b) Radial Velocities

The journal of observations presented in Tables 1 and 2 gives the heliocentric radial velocities of the "best" lines for the first and second series spectrograms, respectively.

TABLE 1

JOURNAL OF ESO OBSERVATIONS*

Plate	J.D. 2 440 000 +	Phase	λ 4686 He II R.V. (kms^{-1})	λ 4686 He II Half intensity width
R 290	2684.60	0.390	-----	1412
P 54	2727.676	0.624	-----	2151
P 314	2973.790	0.399	-----	941
P 383	3083.746	0.106	-----	2017
P 393	3084.630	0.152	-----	2689
P 594	3195.563	0.910	-----	2420
P 728	3284.903	0.547	+ 234	1882
P 729	3285.862	0.597	+ 242	2017
P 741	3286.857	0.648	+ 261	2151
P 750	3287.858	0.700	+ 261	2017
P 761	3288.848	0.752	+ 292	----
P 770	3289.840	0.803	+ 273	2420
P 778	3290.850	0.856	+ 365	2151
P 894	3419.563	0.536	+ 269	1882
P 897	3420.544	0.587	+ 276	1748
P 903	3424.526	0.794	-----	2420
P 969	3537.574	0.662	+ 274	2151
P 972	3538.554	0.713	+ 331	2218
P 992	3567.519	0.216	+ 366	2017
P 1079	3578.519	0.787	+ 272	2151
P 1203 P 1207	3732.773 3732.929	0.798	+ 289	2353
P 1213 P 1219	3733.693 3733.918	0.847	+ 331	2285
P 1224	3734.716	0.894	+ 341	2420
P 1232	3778.599	0.172	+ 322	2420
P 1253	3780.550	0.273	+ 200	2017
P 1262 P 1270	3781.540 3781.883	0.334	+ 226	1412
P 1271	3782.561	0.378	+ 195	1210
P 1280	3783.586	0.431	-----	1479
P 1286	3783.843	0.444	+ 175	1412
P 1288	3784.542	0.481	+ 207	1680
P 1291	3784.841	0.496	-----	1613
P 1292	3785.670	0.539	+ 269	2017
P 1293	3805.514	0.569	+ 287	2017
P 1297	3806.505	0.621	-----	2151
P 1313	3809.513	0.777	+ 329	2353
P 1317	3810.515	0.829	+ 298	2420
P 1320	3811.536	0.882	+ 283	2285
P 1328	3813.543	0.986	+ 259	1748
P 1340	3817.508	0.192	+ 267	2285
P 1352	3819.519	0.296	+ 223	2017

*The phase is based on the ephemeris given by Breysacher and Perrier (1980).

TABLE 2

JOURNAL OF CTIO OBSERVATIONS*

Plate	J.D. 2 440 000 +	Phase	R.V. ($km\ s^{-1}$) H9a	HeIa 4026	Hδa	Hγa	NVe 4604	HeIIe 4686	IS CaII-K
2418(2)	3839.554	0.336	116	89	19	-20	204	103	151
2423(2)	3840.542	0.387	95	-40	-101	-53	210	155	117
2429(2)	3841.608	0.443	74	102	6	-76	---	164	163
2433(2)	3842.539	0.491	-14	23	-5	34	286	193	133
2439(2)	3843.542	0.543	73	10	2	2	217	280	80
2444(8)	3844.542	0.595	79	41	35	-23	230	249	161
2450(8)	3845.547	0.647	53	-4	90	-17	123	364	135
2455(8)	3846.539	0.699	49	100	17	-11	85	273	120
2461(8)	3847.538	0.750	125	-3	23	-61	224	263	106
3072(5)	4137.736	0.813	132	-6	-13	-185	271	266	114
3078(5)	4141.847	0.026	(-143)	13	-120	---	238	248	103
3081(5)	4144.801	0.180	166	212	265	323	104	219	150
3284(2)	4254.569	0.877	69	232	100	15	242	354	39
3289(2)	4255.558	0.929	-61	(-231)	-80	-288	233	378	150
3300(4)	4257.599	0.035	257	118	-207	---	184	228	107
3310(6)	4259.622	0.140	88	248	266	363	280	289	17
3322(4)	4261.589	0.242	225	166	-242	---	321	271	63
3329(6)	4262.639	0.296	157	299	266	250	240	202	81
3341(1)	4265.569	0.448	126	160:	129	---	306:	143	97
3347(1)	4267.553	0.551	212	104	122	306	247	274	112
3350(1)	4269.549	0.655	164	---	-68	{-86 {293	229:	329	88
3353(3)	4270.556	0.707	141	184	86	-167	---	279	74
3356(3)	4271.545	0.758	164	102	132	-83	---	278	99
3360(3)	4272.536	0.810	85	32	100	{-99 {255	240	270	108
3367(2)	4274.549	0.914	108	169	46	253	236	292	86
3370(3)	4275.543	0.966	156	32	-11	253	237	287	99
3374(1)	4276.558	0.019	91	120	39	270	---	230	128
3378(3)	4277.533	0.069	149	128	111	259	439	275	91

*The phase is based on the ephemeris given by Breysacher and Perrier (1980).

The last column of Table 1 refers to the half-intensity width of the λ4686 emission. The phase is calculated according to the ephemeris:

$$(\mathrm{HJD})_0 = 2{,}443{,}158.771 + 19.266.E$$

given by Breysacher and Perrier (1980).

From the 43 spectrograms obtained by J. B. (Table 1), only 33 were suitable for radial velocity determinations, λ4686 He II being furthermore the only line measurable with sufficient accuracy. In Table 2, other emission and absorption lines are included in addition to λ4686. The λ4604 N V line is the next best emission line but hard to measure well because it appears only weakly above the continuum. Among the absorption lines, H9 is the best one, all the other lines being either weak, blended or perturbed by the nebula + W-R emission. In spite of inferior precision, radial velocities are nevertheless also given for the λ4026 He I, Hδ, and Hγ lines.

The radial velocity of the NGC 346 nebula was also determined. A mean value of 170 $km\ s^{-1}$ ($\sigma = 14\ km\ s^{-1}$)

was derived from all the ESO spectrograms listed in Table 1, using the Hβ, λλ4959 and 5007 [O III] lines. These lines and also λ3869 of [Ne III] were measured in the last ten CTIO spectra in Table 2 giving a velocity of 169 ± 3 km s^{-1} for the nebula. The two values are in excellent agreement and compare well with the 163 km s^{-1} derived by Feast (1970) from Hα measurements.

For the interstellar K-Ca II, line the mean radial velocity found from Table 2 is 106 ± 7 km s^{-1}, which is significantly less than the nebular velocity. Feast *et al.* measured 153 km s^{-1}. From high dispersion *IUE* spectroscopy, de Boer and Savage (1980) confirmed that the UV interstellar lines in the spectrum of HD 5980 exhibit maximum absorption near 150 km s^{-1} with, however, the existence of components near 90 and 100 km s^{-1}. In addition, they detected a cloud of unknown origin at 300 km s^{-1}.

c) *Orbital Elements*

Figure 2*a* shows the radial velocity curve obtained for the λ4686 He II line using the period $P = 19^{\rm d}.266$ determined by Breysacher and Perrier (1980). If this emission line reflects the W-R orbit, an assumption which will be discussed later, the following elements are derived:

$\gamma_{\rm W\text{-}R}$(km s^{-1}) $= 255 \pm 8$
$K_{\rm W\text{-}R}$(km s^{-1}) $= 78 \pm 13$
T(JD) $= 2{,}444{,}264.9 \pm 0.5$
$\omega(°)$ $= 190 \pm 14$
e $= 0.49 \pm 0.10$
E_0(JD) $= 2{,}443{,}304.4 \pm 0.7$
σ(km s^{-1}) $= 38.$

E_0 is the time of passage through the γ velocity from negative to positive. This occurs at light curve phase $\phi = 0.56 \pm 0.04$, i.e., $3^{\rm d}.8 \pm 0.7$ after the secondary minimum of the light curve (W-R star in front). This phase shift is more than expected from the eccentric orbit ($1^{\rm d}.4 \pm 0.4$). The excess difference can be understood in terms of an asymmetric distribution of the emitting regions as already proposed by Breysacher and Perrier (1980) to explain the shape of the light curve.

The N V velocity curve, which might better represent the true velocity of the W-R star, is unfortunately too noisy to be useful.

Considering now the O-star orbit, the H9 and λ4026 He I absorption lines (Fig. 2*b*) go practically in antiphase with the λ4686 He II emission but with negligible phase shift relative to the light curve ephemeris. The period and the eccentricity being fixed to $P = 19^{\rm d}.266$ and $e = 0.49$ respectively, the following values are derived for the mean of H9 and λ4026 He I:

γ_0(km s^{-1}) $= 113 \pm 8$
K_0(km s^{-1}) $= 69 \pm 16$
T(JD) $= 2{,}443{,}162.0 \pm 0.8$
$\omega(°)$ $= 345 \pm 21$
E_0(JD) $= 2{,}443{,}159.6 \pm 1.0$
σ(km s^{-1}) $= 24.$

We note that the difference between the times of periastron passage as determined from the λ4686 emission and absorption line orbits is 57.25 ± 0.05 orbital cycles, which is not an integer $+0.5$. This is mainly due to the fact that the difference in ω values of the two orbits is not exactly 180°. The Hγ line shows two components, possibly created by splitting from an unclearly seen nebular emission (there is a relatively strong nebular emission at Hβ). In the phase[4] interval $0.0 < \phi < 0.2$ the negative component is not seen and may be masked by a blueshifted emission component.

From the above determined quantities one finds the masses:

$$M_{\rm W\text{-}R} \sin^3 i = 2.0 \pm 1.0\, M_\odot$$
$$M_0 \sin^3 i = 2.2 \pm 1.1\, M_\odot\ .$$

With the inclination i deduced from the light curve analysis close to 80°, these masses are extremely low considering the high luminosities of the stars. If one looks to other (better behaved) double-lined binary systems with WN type components (see Moffat and Seggewiss 1980; Massey 1981; Moffat 1981; Niemala 1981), an $M_{\rm W\text{-}R}/M_{\rm OB}$ ratio of the order of 0.3–0.4 falls in the range of the values determined for WN4 binaries. Assuming that the $K_{\rm W\text{-}R}$ value for HD 5980 has been reduced by perturbations and taking $K_0/K_{\rm W\text{-}R}' = 0.3$, where $K_{\rm W\text{-}R}'$ is the true orbital semiamplitude, we then obtain:

$$K_{\rm W\text{-}R}' = 230 \text{ km s}^{-1}$$

and

$$M_{\rm W\text{-}R}' \sin^3 i = 8\, M_\odot\ ; \quad a_{\rm W\text{-}R}' \sin i = 76\, R_\odot$$
$$M_0' \sin^3 i = 27\, M_\odot\ ; \quad a_0' \sin i = 23\, R_\odot\ .$$

The mass of the O-star now appears to be more realistic, although it may still be somewhat low for its spectral type, as expected if this star has evolved from the main sequence by mass loss (see § IV). However, it remains to be explained why such a large $K_{\rm W\text{-}R}'$ is not seen, in particular for the λ4604 N V emission line; possibly the same kind of perturbations occur for it too. The orbital radii are not extraordinarily small.

d) *Profile Changes*

Figure 3 illustrates typical phase-dependent variations of the λ4686 He II line profile for the three plates of 1979 September. The width changes are much larger than the radial velocity shifts due to the orbital motion; this supports our assumption above that the W-R orbit obtained from the λ4686 He II line probably does not reflect the true motion of the W-R star.

Figure 4 shows a plot of the total width of λ4686 at half height versus phase, for all ESO and CTIO observations. For the first series of spectrograms on electronographic emulsion, this corresponds to half-intensity measurements, while for the second series of spectrograms, because of uncalibrated plates, it refers to half photographic density (i.e., half log intensity to a good approximation). The fit of both sets of data (Fig. 4)

[4] If not explicitly mentioned, the light curve phase is considered.

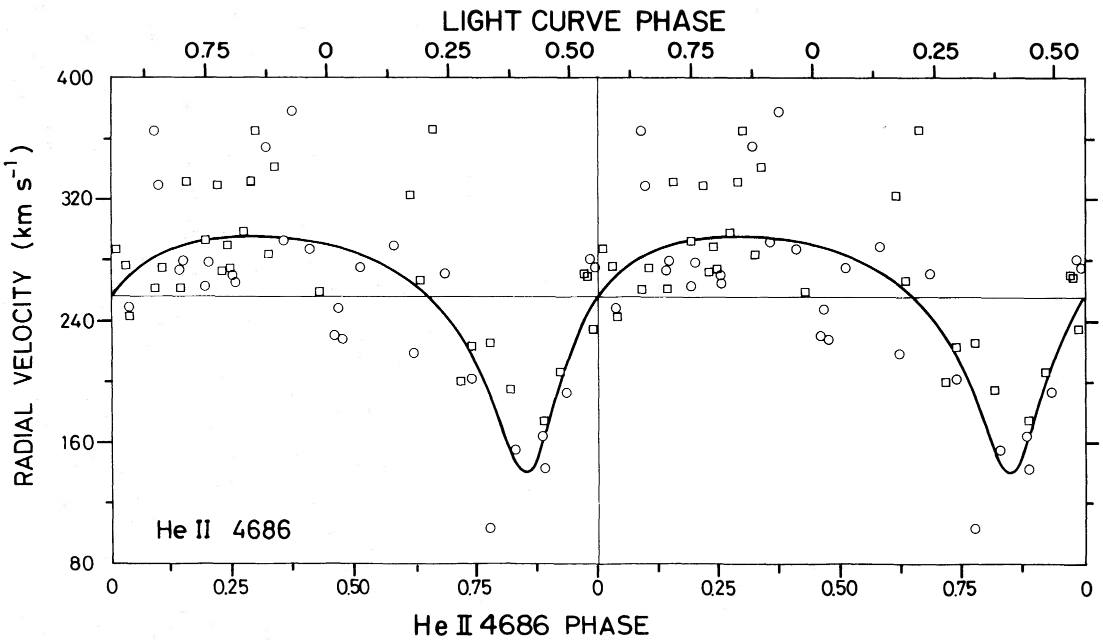

FIG. 2*a*

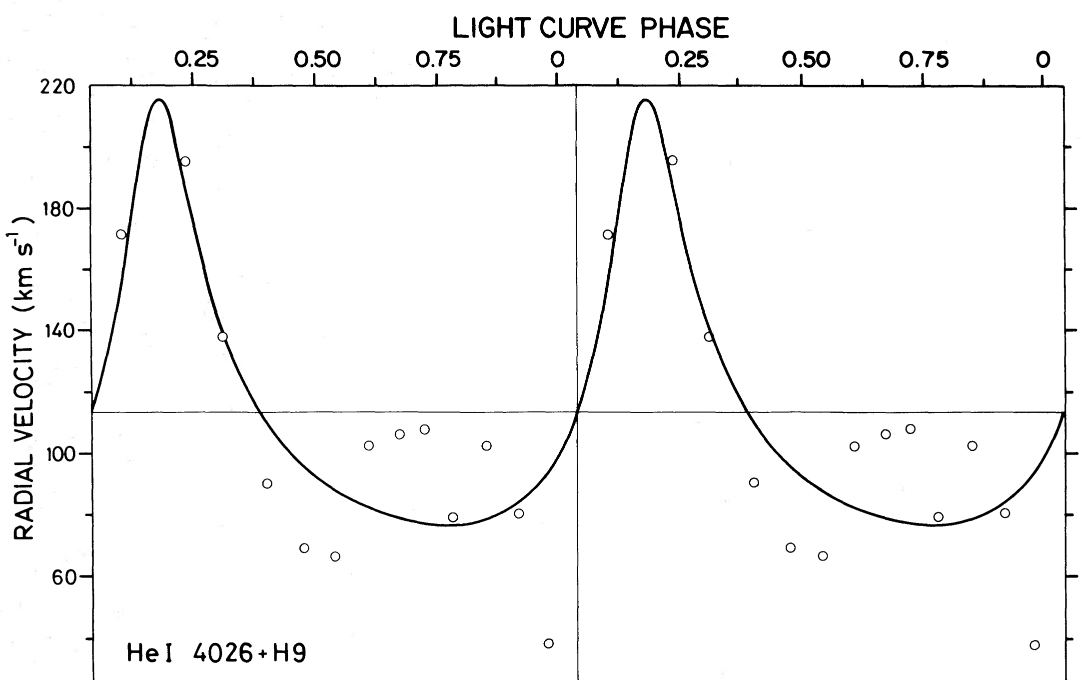

FIG. 2*b*

FIG. 2.—(*a*) Phased data and orbit according to the formal least-squares fit to the He II 4686 emission line. Phase zero for λ4686 (passage through the γ-velocity from negative to positive) corresponds to the light curve phase 0.56 $\pm$ 0.04. Squares refer to the ESO data in Table 1; circles to the CTIO data in Table 2. (*b*) Phased data and orbit according to the formal least-squares fit to the mean absorption (H9 and He I 4026). The observations are drawn from Table 2 and refer to running averages in JD and in radial velocity of four values per bin with double overlap. Phase zero for the absorption (passage through the γ-velocity from negative to positive) corresponds to the light curve phase 0.04 $\pm$ 0.05.

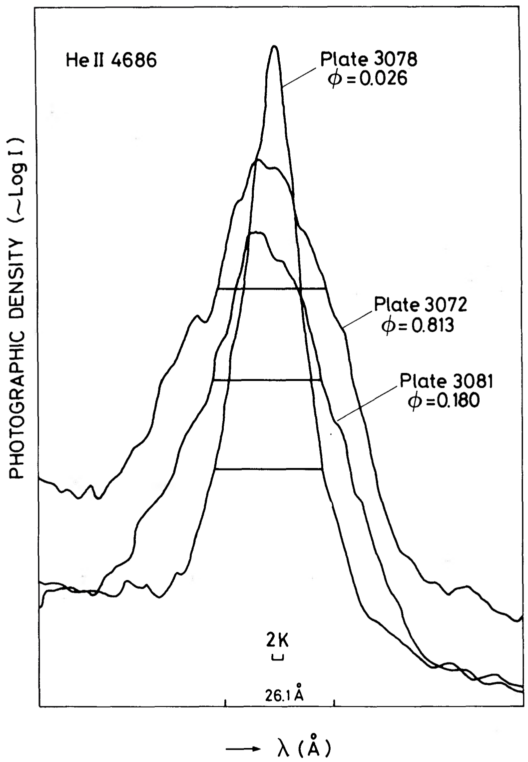

FIG. 3.—Typical PDS density scans of He II 4686 showing phase dependent variations in width. Phases refer to the light curve. Radial velocities were obtained from fitting a parabola to the inner 26 Å. The full velocity amplitude ($2K$) is shown for comparison.

reveals a sharp deep minimum at $\phi = 0$ and a broad, shallow minimum around $\phi = 0.35$, i.e., at the primary and secondary light curve minima, respectively.

IV. DISCUSSION

The present spectroscopic study has undoubtedly brought important new information about the SMC W-R binary HD 5980; however, a clear picture of this system is still difficult to derive. A number of facts remains to be explained; we will comment on them in what follows.

A first remark concerns the period and the eccentricity of the orbit which seem to be well established from both the photometric and spectroscopic observations. Moffat and Seggewiss (1980) have noted that the eccentricity e is significantly different from zero only for W-R binaries with relatively long periods ($P \geq 50^d$). This is readily understood since, in a short period system, interaction effects will quickly act to circularize the orbit. Two galactic W-R binaries (HD 50896 and HD 197406) with suspected compact companions appear to have at the same time an appreciable orbital eccentricity and a period of a few days only (see Moffat and Seggewiss 1980; Massey 1981). Because of its double-lined spectral behavior and its light curve, the present object can hardly be of this type. With $P \sim 19^d$, HD 5980 is thus the first moderately short period double-lined O + W-R star binary to show a strongly eccentric orbit.

The second puzzling point is the low values that are obtained for the masses when no particular assumption is made about the low velocity amplitude of the λ4686 He II emission line. The bright absolute magnitude and

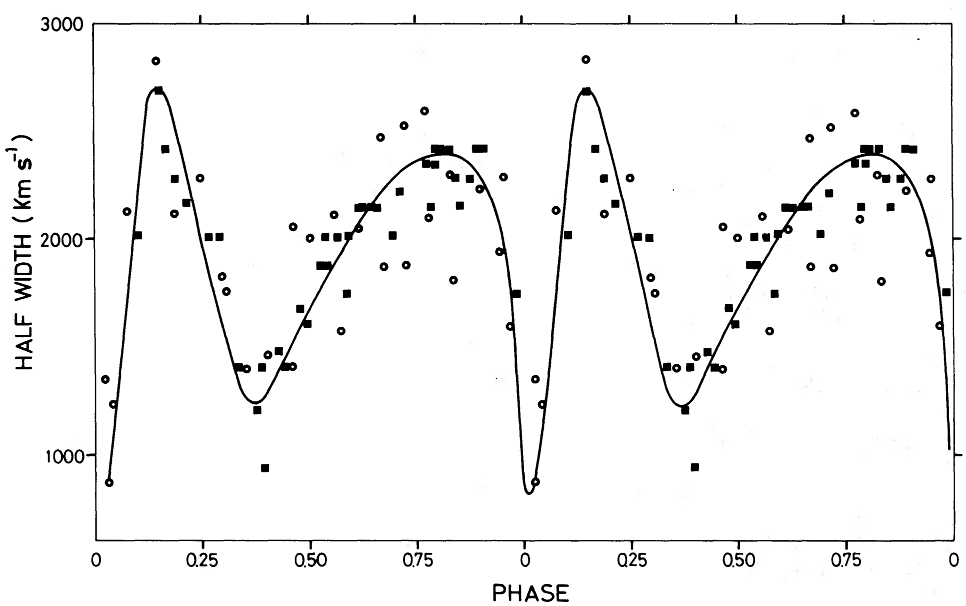

FIG. 4.—Full half width versus light curve phase for the emission line He II 4686. The CTIO data (*circles*) refer to half density (~log density) width and have been adjusted to match the ESO data (*squares*) based on full widths at half intensity.

the eclipse light curve of HD 5980 cast doubt on the reality of such small masses. This implies that the λ4686 He II radial velocity curve likely does not represent the true motion of the W-R component. To understand why, the origin of the phase-dependent variations exhibited by the He II emission line deserves particular attention.

From the light curve, Breysacher and Perrier (1980) inferred the presence of a brighter zone on the side of the W-R envelope facing the O star which could plausibly be caused by the interaction of the O star wind with the outer regions of the W-R envelope. This is supported by the present spectroscopic observations, as follows. The existence of a strong stellar wind from the O7 I: component of HD 5980 is inferred from the observed radial velocity gradient of the Balmer lines (Fig. 5), generally interpreted as outward accelerated motion (Hutchings 1970). Possibly the O component has emission of its own like the nearby Of supergiant Sk 80. Supposing that the W-R envelope, the brightened region, and also the O star each contribute to the λ4686 emission feature, the observed width variations (Fig. 4) can be interpreted in the following way. At $\phi = 0$, there is a significant variation of the color indexes $\Delta(b - y)$ and $\Delta(u - b)$ which indicates that during the primary eclipse the b magnitude behaves differently from the u and y magnitudes which mainly refer to the continuum. Since the b filter is almost centered on the strong λ4686 He II emission line which, as stressed by Conti (1975) "can be in emission only in an envelope," the observed color effect suggests that when the O star is in front, the λ4686 emitting region, or at least part of it, still remains visible. At this time, the brighter zone of the W-R envelope is fully eclipsed, and only a narrow emission component is seen. Due to the eccentricity of the orbit, around periastron (light curve phase 0.17 ± 0.04) the interaction effect is strongest, the brighter zone is again visible, and the λ4686 line reaches its maximum width. At the secondary minimum (W-R star in front), the brightened region of the W-R envelope is not visible to us, and again the λ4686 line gets narrower. During the eclipses, the λ4686 emission components from the O star and the W-R star overlap, so that this line remains narrow in accordance with the above proposed interpretation.

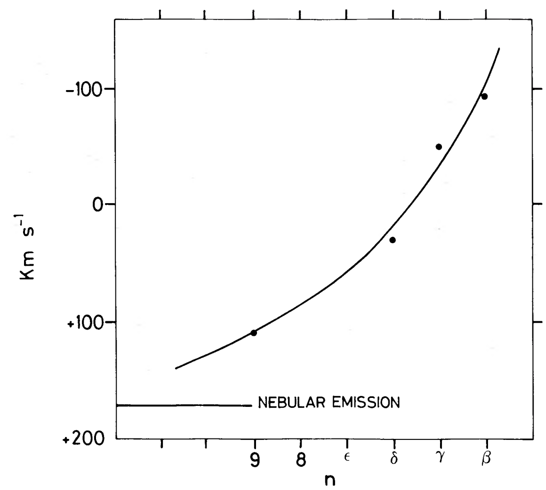

FIG. 5.—Radial velocity gradient of the Balmer absorption lines from the O7 I: component. The mean velocity of He I 4026 is identical to that for H9. A hand-drawn curve indicates the velocity trend which approaches the nebular value asymptotically. Although Hβ absorption is not seen in Fig. 1, it was measurable on the lower noise IIIa-J plates.

A multicomponent λ4686 emission feature also explains nicely the reduced $K_{\text{W-R}}$ value one observed as well as the equivalent width variations reported by Breysacher and Westerlund (1978).

We thank R. Mendez for taking three plates (1979 September). J. B. is grateful to Messrs. P. Giordano and A. Torrejon for their assistance in the operation of the "caméra électronique" and to the staff of the C.D.C.A. for their help during the measurements of the spectra. A. F. J. M. is grateful to C. T. Bolton and R. Lyons for time and assistance on the PDS at the David Dunlap Observatory and to the Natural Sciences and Engineering Research Council of Canada for financial aid. A. F. J. M. and V. S. N. extend warm thanks to the staff at CTIO for their never-failing hospitality and assistance.

REFERENCES

Azzopardi, M., and Breysacher, J. 1979, *Astr. Ap.*, **75**, 120.
Baranne, A., and Duchesne, M. 1976, *Adv. Electronics Electron Phys.*, **40B**, 641.
Breysacher, J. 1981, *Astr. Ap. Suppl.*, **43**, 203.
Breysacher, J., and Perrier, C. 1980, *Astr. Ap.*, **90**, 207.
Breysacher, J., and Westerlund, B. E. 1978, *Astr. Ap.*, **67**, 261.
Conti, P. S. 1975, *Mém. Soc. Roy. Sci. Liège*, 6ième Sér., **9**, 193.
de Boer, K. S., and Savage, B. D. 1980, *Ap. J.*, **238**, 86.
Feast, M. W. 1970, *M.N.R.A.S.*, **149**, 291.
Feast, M. W., Thackeray, A. D., and Wesselink, A. J. 1960, *M.N.R.A.S.*, **121**, 337.
Hoffmann, M., Stift, M. J., and Moffat, A. F. J. 1978, *Pub. A.S.P.*, **90**, 101.
Hutchings, J. B. 1970, *M.N.R.A.S.*, **147**, 161.
Massey, P. 1981, *Ap. J.*, **246**, 153.
Moffat, A. F. J. 1981, in *IAU Colloquium 59, Effects of Mass Loss on Stellar Evolution*, ed. C. Chiosi and R. Stalio (Dordrecht: Reidel), p. 301.
Moffat, A. F. J., and Seggewiss, W. 1980, in *IAU Symposium 88, Close Binary Stars: Observations and Interpretation*, ed. M. J. Plavec, D. M. Popper, and R. K. Ulrich (Dordrecht: Reidel), p. 181.
Niemela, V. S. 1981, in *IAU Colloquium 59, Effects of Mass Loss on Stellar Evolution*, ed. C. Chiosi and R. Stalio (Dordrecht: Reidel), p. 307.
Smith, L. F. 1968*a*, *M.N.R.A.S.*, **138**, 109.

Smith, L. F. 1968*b*, *M.N.R.A.S.*, **140**, 409.
———. 1973, *IAU Symposium 49, Wolf-Rayet and High Temperature Stars*, ed. M. K. V. Bappu and J. Sahade (Dordrecht: Reidel), p. 15.
Swings, P., and Jose, P. D. 1950, *Ap. J.*, **111**, 513.
Walborn, N. R. 1977, *Ap. J.*, **215**, 53.
———. 1978, *Ap. J.* (*Letters*), **224**, L133.

JACQUES BREYSACHER: European Southern Observatory, Karl-Schwarzschild-Strasse 2, 8046 Garching bei München, Federal Republic of Germany

ANTHONY F. J. MOFFAT: Département de Physique, Université de Montréal, C.P. 6128, Succ. "A," Montréal, Qué. H3C 3J7, Canada

VIRPI S. NIEMELA: Instituto de Astronomía y Física del Espacio, Casilla de Correo 67, Suc. 28, 1428 Buenos Aires, Argentina